Received: 10 June 2025 | Revised: 28 July 2025 | Accepted: 12 August 2025 | Published online: 2 September 2025

Smart Wearable Technology
2025, Vol. 00(00) 1–11
DOI: 10.47852/bonviewSWT52026420

REVIEW

The Recent Advancements to Measure the Blood Pressure Using Photoplethysmography, Electrocardiogram, and Microchannel

Hajar Danesh[1,*], Hamidreza Shirzadfar[1,*], Mahla Manian[1] and Melika Pazhom[1]

[1]*Department of Electrical and Biomedical Engineering, Faculty of Engineering and Technology, Shahid Ashrafi Esfahani University, Iran*

Abstract: Uncontrolled blood pressure poses significant health risks, making accurate measurement essential in healthcare. Conventional blood pressure measurement methods, typically using inflatable cuffs, can cause patient discomfort, tissue damage, and are unsuitable for long-term monitoring. Consequently, researchers are exploring noninvasive, cuffless methods that provide continuous and accurate blood pressure assessment. This article presents a comprehensive review of sensors and estimation models used in cuffless blood pressure monitors, with a focus on enhancing accuracy and minimizing calibration requirements. A literature search was conducted using Google Scholar and reputable journals, including *IEEE*, *Frontiers*, and *MDPI*, resulting in the selection of 35 relevant studies. The review examines innovative techniques based on electrical, mechanical, and optical sensors. Particular attention is given to photoplethysmography (PPG), electrocardiography (ECG), and bioimpedance (Bio-Z), which, when combined with advanced signal analysis and deep learning models, show promising results. PPG enables blood volume measurement at accessible sites like the fingertip or wrist, leveraging parameters such as pulse transit time. ECG, which directly reflects heart activity, is also widely used for blood pressure estimation. Recent advancements in machine learning have improved accuracy, with models such as HGCTNet (a hybrid CNN-Transformer architecture) achieving an error margin of 0.9 ± 6.5 mmHg for diastolic and 0.7 ± 8.3 mmHg for systolic blood pressures. Despite the potential, challenges remain, including the need for continuous calibration of PPG-based systems. Ongoing research aims to address these limitations by improving signal quality and developing robust algorithms. The demonstrated accuracy and reduced calibration requirements suggest that cuffless blood pressure monitoring technologies may soon become viable for widespread clinical and home use.

Keywords: blood pressure, medical sensor, monitoring, machine learning, PPG

1. Introduction

High blood pressure is one of the factors that can lead to stroke and heart disease [1]. Therefore, measuring this vital parameter is of great importance, as high blood pressure is one of the primary causes of heart disease and stroke. Controlling it can reduce the risk of these conditions by 10% to 20% [2] and ultimately can help prevent an increase in mortality rates [3]. Thus, it is essential to continuously and regularly monitor individuals' blood pressure. In general, three types of parameters are reported in blood pressure measurement: systolic blood pressure (SBP), diastolic blood pressure (DBP), and mean arterial pressure (MAP). From Equation (1), the arterial pressure is calculated [4].

$$MAP = \frac{SBP + 2DBP}{3} \tag{1}$$

In recent years, with advancements in technology for measuring blood pressure, more diverse and sensitive methods have been introduced. In the 1800s, blood pressure measurement was performed using invasive arterial cannulation [5]. Although this invasive method was uncomfortable for patients, it is still used in the intensive care unit (ICU) for continuous blood pressure monitoring [6]. Today, noninvasive blood pressure measurement techniques are common in healthcare standard practices in clinics. These methods are based on a plastic inflatable cuff that, when pressure is applied to the brachial artery, occludes blood flow in that artery; then, by releasing the pressure in the cuff and monitoring the radial pulse through palpation or by listening to Korotkoff sounds using a stethoscope, blood pressure is measured in both systolic and diastolic phases. Measuring blood pressure with a mercury sphygmomanometer and based on the auscultation of Korotkoff sounds has become the gold standard due to its high accuracy; however, due to the prohibition of using mercury sphygmomanometers, the use of this technique has significantly decreased [7]. In the use of an inflatable cuff, the pressure applied to the patients' arms can cause discomfort, and in continuous and prolonged measurements, it may lead to tissue damage. Today, there are various methods for estimating blood pressure. One

*Corresponding authors: Hajar Danesh, Department of Electrical and Biomedical Engineering, Shahid Ashrafi Esfahani University, Iran. Email: h.danesh@ashrafi.ac.ir and Hamidreza Shirzadfar, Department of Electrical and Biomedical Engineering, Shahid Ashrafi Esfahani University, Iran. Email: hsh@ashrafi.ac.ir

common method for estimating blood pressure is the pulse transit time (PTT). The PTT refers to the time it takes for the pulse wave generated by the heartbeat to travel from the heart to the sensor of the measuring device. PTT can be obtained using various methods, such as utilizing photoplethysmography (PPG) signals, electrocardiography (ECG) signals, or bioimpedance (Bio-Z) [8, 9]. In the PPG technique, an optical sensor is used to generate the PPG signal. This signal contains very useful information, including blood oxygen levels, heart rate, blood volume changes, etc., which can help estimate blood pressure based on the information obtained from this signal. Generally, the optical sensor consists of an infrared light-emitting diode (LED) for emitting light and a photodetector. The infrared light can generate the PPG signal either by reflecting off the epidermis or by passing through it [10]. After receiving the PPG signal, blood pressure must be estimated based on the characteristics of the signal and using various methods. Another signal related to blood pressure is the ECG signal. In general, three factors affect changes in blood pressure: heart contraction, blood volume, and peripheral resistance. Among these factors, heart contraction can be examined using ECG signals [11]. Therefore, some studies utilize a combination of data from both ECG and PPG signals to estimate blood pressure [12]. To employ this method, two PPG sensors or one PPG sensor and one ECG sensor must be used, which represents a hardware requirement and is considered a drawback of this method [13]. Additionally, since physiological parameters vary among individuals, the use of the PPT method requires calibration for each patient, thus it makes personalization necessary, which is another limitation of this approach [14]. Bio-impedance (Bio-Z) refers to the impedance of tissues against the current applied to them, which can be used to measure body fluid volumes, such as blood volume in vessels [15]. Nowadays, researchers are seeking methods to estimate blood pressure that do not require specific calibration for each patient. Recent studies have employed methods such as machine learning (ML) algorithms and, in particular, deep learning (DL) algorithms for blood pressure estimation.

2. Literature Review

In recent years, cuff-less blood pressure estimation methods using biosignals such as PPG and ECG have received increasing attention. This section highlights several key studies from 2010 to 2021 that employed ML and DL techniques for estimating blood pressure without the use of a cuff. Yoon et al. [16] in 2009 utilized ECG and PPG signals to extract pulse arrival time (PAT) and applied a linear regression model for blood pressure estimation. Their method achieved a correlation coefficient of $r = -0.76$ and a relative error ranging from 4% to 11% in estimating both systolic and diastolic blood pressures. Kurylyak et al. [17] in 2013 employed a feedforward artificial neural network (ANN) trained with 21 features extracted solely from the PPG signal. The model achieved a mean absolute error (MAE) of 3.80 ± 3.46 mmHg for systolic and 2.21 ± 2.09 mmHg for diastolic blood pressures. Sun et al. [18] in 2016 proposed a multivariate linear regression model using 18 features including PAT. Their dataset was recorded during exercise using ECG and PPG. The model yielded a mean error of 0.43 mmHg and a standard deviation of 13.52 mmHg with a correlation of $r = 0.86$r for systolic blood pressure estimation. Tanveer and Hasan [19] introduced a hybrid DL model based on ANN and LSTM architectures using ECG and PPG. The model demonstrated excellent performance with MAE = 1.10 mmHg and RMSE = 1.56 mmHg for systolic blood pressure, meeting both AAMI and British Hypertension Society (BHS) standards. Leitner et al. [20] in 2022 proposed a blood pressure estimation model using only PPG signals, integrating DL architectures composed of convolutional neural networks (CNN) and recurrent neural networks (RNN). A key feature of their method is the application of transfer learning to enable personalized blood pressure estimation. In this approach, a general model is first trained on a large dataset from multiple individuals and then fine-tuned using a small amount of personal data (approximately 50 samples per subject). The personalized model achieved an MAE of 3.52 mmHg for systolic blood pressure and 2.20 mmHg for diastolic pressure, meeting the standards of both AAMI and BHS. By relying solely on PPG signals, this method enhances practicality for real-world applications, particularly in wearable devices. This study demonstrates that personalization through transfer learning can significantly improve accuracy, even with limited subject-specific data. It highlights the potential of DL models to generalize well across individuals while allowing lightweight personalization for more precise cuff-less blood pressure monitoring.

This article examines the latest advancements in sensor types in cuffless blood pressure monitors and blood pressure estimation models. The findings of this article can significantly contribute to future studies in this field.

3. Materials and Methods

This paper reviews the latest methods and developments in the design and construction of cuffless blood pressure monitors. Selected articles utilizing new technologies, a combination of suitable sensors, and the application of novel methods for blood pressure estimation, such as DL, have achieved promising results. Most of these articles have been selected from those published since 2020 to the present. Additionally, the search was conducted using phrases such as “cuffless sphygmomanometer,” “PPG sensor in cuffless blood pressure measurement,” “ECG sensor in cuffless sphygmomanometer,” “bioimpedance sensor in cuffless sphygmomanometer,” and “deep learning in blood pressure estimation” on the Google Scholar platform and from reputable journals such as *IEEE*, *Frontiers*, *MDPI*, *PubMed*, and *Nature*. Figure 1 shows the flowchart of the article selection process.

3.1. Study the principles of essential sensors to measure of blood pressure

The various sensors have been proposed for measuring blood pressure without the use of a cuff. In this section, these sensors are categorized based on the physical nature that relates a parameter directly or indirectly to blood pressure. The mechanical sensors directly sense blood pressure, electrical sensors detect certain electrical signals associated with blood pressure received from the body, and optical sensors focus on the PPG sensor among these sensors.

Pressure-based mechanical sensors are used in blood pressure measurement based on inflatable cuffs, which respond directly to pressure due to their structure and generate electrical signals. Generally, there are four types of flexible mechanical sensors: piezo-capacitive, piezo-resistive, piezoelectric, and triboelectric sensors. In capacitive piezoelectric sensors, the pressure caused by blood flow leads to a change in the capacitance of the pressure sensor, and this change in capacitance is converted into an electrical signal. Resistive piezo sensors experience a change in resistance due to the applied pressure, resulting in the generation

Figure 1
The block diagram of the study methodology

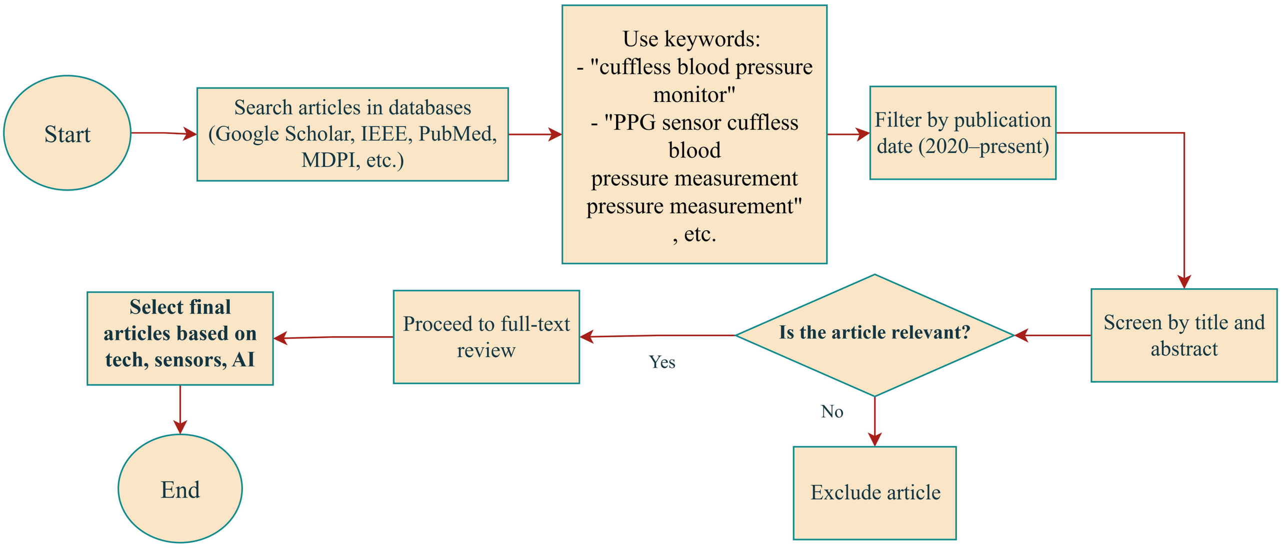

of an electrical signal. Piezoelectric sensors operate based on the piezoelectric effect, such that under stress or strain from blood pressure, a potential difference is created between two electrodes due to the properties of the dielectric material. By measuring this potential difference, blood pressure can be directly measured. Triboelectric sensors are also based on electrostatic induction, where external pressure on the electrodes induces charges through an external circuit, ultimately resulting in an electrical output that indicates pressure. However, unfortunately, the use of such sensors is not recommended because their measurement is limited, and they produce very weak signals; thus, it is not feasible to use these types of sensors effectively while applying the constraints of “non-invasive” and “without a cuff” [21]. Figure 2 presents the structure of the aforementioned mechanical sensors [21]. Resistive and capacitive sensors require an external power source for measurement, while piezoelectric and triboelectric sensors can directly convert pressure or strain into an electrical signal for self-measurement. The piezoresistive sensors used by the piezoresistive effect, where pressure changes a material’s resistance, altering the output signal. Other sensors detect resistance, capacitance, or charge changes for measurements. Resistive/capacitive sensors need external power, while piezoelectric/triboelectric sensors are self-powered (Figure 2(a)). The capacitive sensors detect pressure (Figure 2(b)) via capacitance changes ($C = Es/d$). The applied pressure shifts plate distance/area, enabling measurement. Figure 2(d) shows triboelectric sensors convert pressure to electricity via contact charging between dissimilar materials, generating measurable current.

Table 1 compares mechanical, electrical, and optical sensors from a technical perspective. Pressure-based sensors are intelligently and specifically designed, as discussed in the following mechanisms. Ion et al. [22] developed a microfluidic-based sensor for recording blood pressure waveforms, which includes a microfluidic channel between two polymer layers filled with an electrolyte solution. One of the layers is covered by a metallic transducer. When this structure is placed on a human wrist, the pulse pressure is sensed through changes in the shape of the microfluidic channel, and the blood pressure waveform is recorded by the transducer. In fact, the applied pressure is calculated by the deformation of the channel membrane and, consequently, the changes in resistance of the microfluidic layer, which depend on the height of the microchannel. The relationship between the applied pressure and the sensor’s resistance can be theoretically calculated. This method has shown high sensitivity in measuring blood pressure in the range of 0 to 150 mmHg, approximately 57 ohms per mmHg for this range. Figure 3 illustrates the schematic of the microfluidic sensor and its use in a wristband placed over the radial artery for measuring blood pressure in the constructed sample [22].

The optical sensors in cuffless blood pressure monitors have always focused on photoplethysmography (PPG) sensors. This sensor is based on the PPG technique, which measures the effect of arterial blood on the intensity of transmitted light in the tissue [23]. This technique follows Beer-Lambert’s law, whereby light emitted from an LED, which can be in red, green, blue, or infrared spectrum, is absorbed by blood within the tissue. Consequently, considering the pulse effect in the artery, during systole, the blood volume in the artery reaches its maximum, while during diastole, the volume is lower. As a result, during cardiac systole, the amount of light absorption is high, and therefore, the transmitted or reflected light is at its lowest. Conversely, during cardiac diastole, light absorption is low, and the transmitted or reflected light from the tissues is at its highest and presented in Figures 4 [24] and 5.

Thus, the generated PPG signal has an AC component that reflects the pulsatile arterial blood and a DC component that represents other tissues such as skin tissues, venous blood, and non-pulsatile arterial blood. Therefore, by analyzing the characteristics of the AC component of this signal, information about the blood can be obtained [25]. Figure 6 presents the components of a PPG signal.

The electrical sensors are another type of monitoring sensor that are significant in measuring biological signals. These sensors are typically electrodes that record the potential difference on the skin’s surface relative to a ground or another electrode. Additionally, in some cases, electrical stimulation may occur prior

Figure 2
The several mechanical pressure measurement sensors: (a) piezoresistive sensors, (b) capacitive sensors, (c) piezoelectric sensors, and (d) triboelectric sensors convert pressure to electricity via contact charging between dissimilar materials, generating measurable current

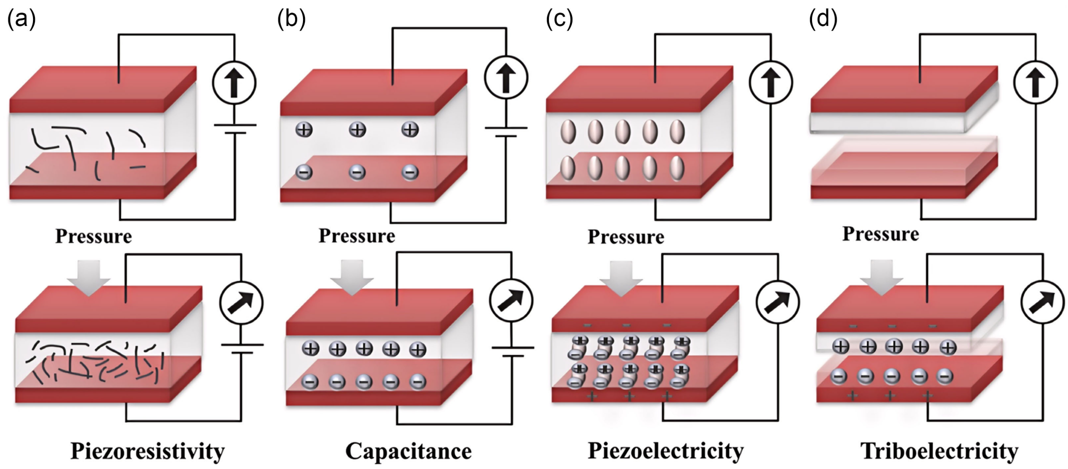

Table 1
Comparison of mechanical, electrical, and optical sensors

Sensor	The Basis of Measurement	accuracy	The Main Advantage	Technical Challenge	Calibration	Energy Consumption
PPG	Changes in light absorption by blood	average	Portable and suitable for daily use, for example as a ring	Errors in skin color and movement	high	low
Microchannel	Deformation of a liquid filled channel under pressure	great	Very high sensitivity	Sealing and preventing liquid leakage	very low	very low
ECG	Electrical activity of the heart	good	High accuracy in detecting heartbeat timing	Electrical noise	average	average
Bio-Z	Tissue resistance to electric current	good	Better deep tissue penetration	Temperature effects on resistance	low	high

to recording this potential difference using another pair of electrodes. The conventional sensors with electrical functionality are ECG electrodes. These sensors generate ECG signals based on the electrical activity of the heart. The integration of information obtained from both ECG and PPG signals provides valuable data for estimating blood pressure. Therefore, ECG sensors can be used alone or in conjunction with PPG sensors for the indirect measurement of blood pressure. Simjanoska et al. [26] utilized three-lead Cooking Hacks ECG sensors to evaluate 16 individuals, three-lead 180 eMotion FAROS ECG sensors for the assessment of 3 individuals, and the single-lead Zephyr Bioharness module ECG biosensor for the evaluation of 25 individuals. Additionally, the heart rate of 7 individuals was studied using the Charis Physionet database. ML was then employed to estimate blood pressure. In the preprocessing stage, the ECG was divided into 30-second segments, and various features such as complexity, fractal dimensions, and entropy were extracted. The entropy of the signal is the number of bits needed to describe a signal [27]. The signal entropy is commonly used in error detection in process control and in the assessment of physiological signals for health monitoring. In most cases, a decrease in entropy indicates the presence of a disease. If pi represents xi consequence x, entropy is calculated as follows:

$$Entropy = \sum_{i=0}^{N-1} pi\ log\left(\frac{1}{pi}\right) \tag{2}$$

The fractal dimensions also refer to measuring the complexity of a signal based on quantifying fractal dimensions. Fractal dimensions also refer to measuring the complexity of a signal based on quantifying the dimensions of fractals. In fact, fractals are mathematical objects with noninteger dimensions, and the concept of fractal dimension has been extended to the analysis of time series. By using fractal dimension, hidden fundamental patterns can be expressed by comparing and magnifying different sections [28]. In the aforementioned article, algorithm has been used to calculate the fractal dimension:

$$X_k^m : x(m), x(m+k), x(m+2k), \ldots, x\left(m + \left\lfloor \frac{N-m}{k} \right\rfloor k\right) \tag{3}$$

The length of the curve X_k^m, $l(k)$ is calculated as

$$l(k) = \frac{\left(\sum_{i=1}^{\lfloor N-m/k \rfloor} |x(m+ik) - x(m+(i-1)k)|(N-1)\right)}{\left(\lfloor \frac{N-m}{k} \rfloor\right)k} \tag{4}$$

Figure 3
The microchannel sensor: (a) the schematic of microchannel sensor including microfluidic channels filled with electrolyte liquid and (b) the fabricated sample of the pressure gauge and sensor placement in the wristband

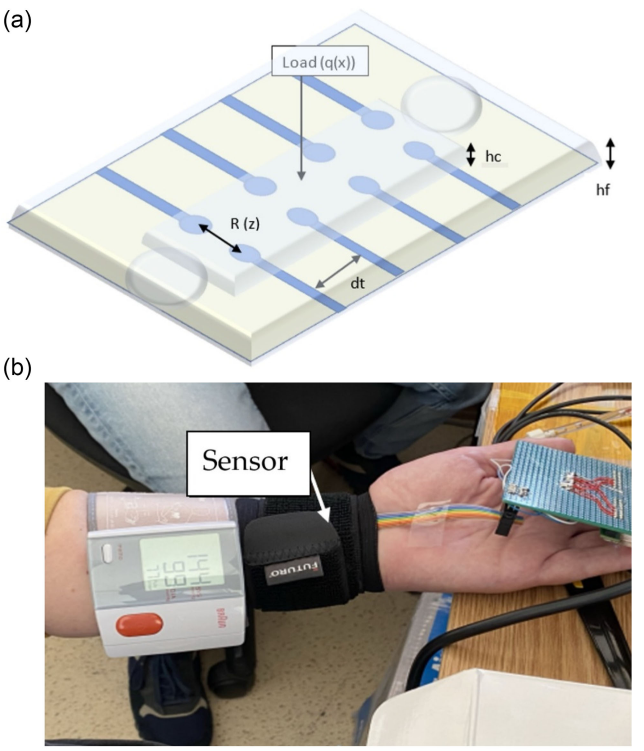

Figure 4
The PPG sensor and photodetector in reflective mode

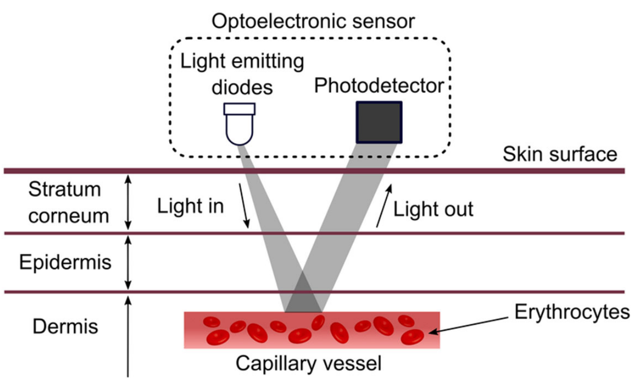

Figure 5
The light reflected or transmitted through the blood as affected by each phase of the cardiac cycle and the volume of blood in the artery

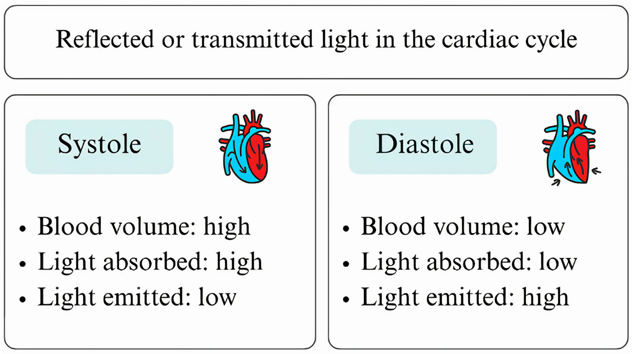

Figure 6
The PPG signal and its components

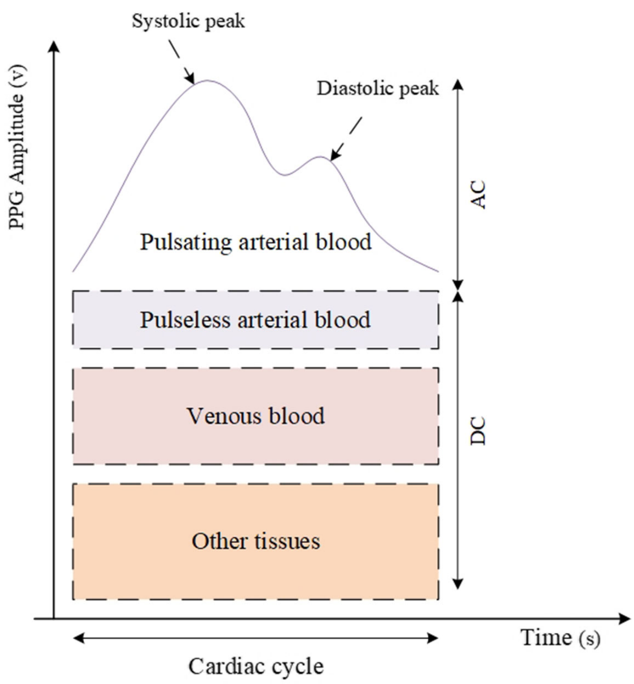

and entropy are two nonlinear features commonly used in ECG signal analysis for blood pressure estimation. Fractal dimension captures the morphological complexity and self-similarity of ECG signals, reflecting structural changes linked to cardiovascular dynamics. Entropy measures the irregularity and unpredictability of heart rate variability, offering insight into autonomic nervous system activity. Both features have shown strong correlation with blood pressure trends in recent studies and are often combined to improve the model accuracy.

Furthermore, considering the established blood pressure ranges for DBP and SBP in medicine, labeling was performed, resulting in three classes: "normal," "prehypertension," and "hypertension," which were designated as 0, 1, and 2, respectively. Simjanoska et al. [26] achieved an accuracy of 85.71%, with an error of 7.86 mmHg for SBP, an error of 6 mmHg for DBP, and a correlation coefficient of 0.77. Ibrahim and Jafari [29] used a low-cost and easy-to-manufacture array consisting of three columns of Bio-Z sensors. In their operational model, the researchers utilized a 6×8 array of silver electrodes in the form of a wristband, with each electrode measuring 5 mm × 5 mm and a distance of 3.2 mm between each electrode and its adjacent one. This is a noninvasive technique that generates a Bio-Z signal by injecting AC signals into the body through one pair of electrodes and sensing the potential difference on the other pair. The phase and measured voltage signal are modulated, and based on the characteristics of

Figure 7
The Bio-Z sensor array

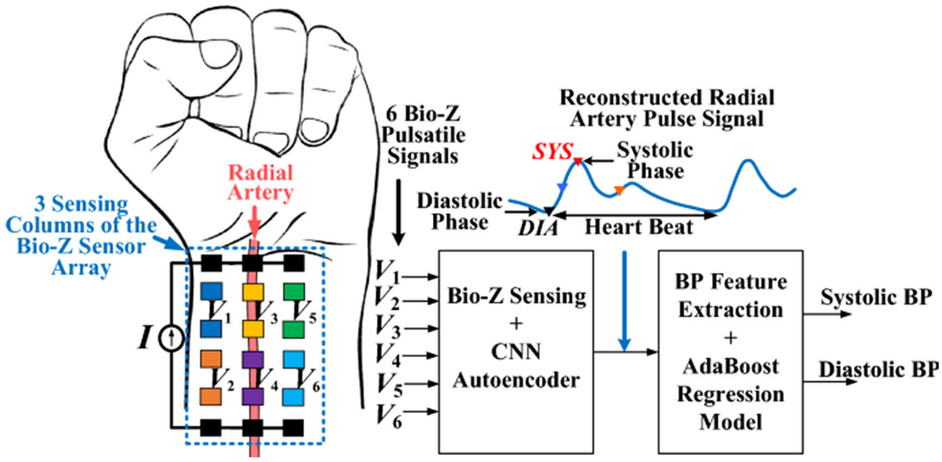

the signal, the behavior of the body and living tissues can be identified. This method's advantage over PPG lies in its ability to penetrate signals deep into the tissue and access the main arteries of the wrist for recording their impedance characteristics. After the signal is received by the electrodes, the DC component is removed in the first stage to estimate the signal for preprocessing. Then, the peak points for each pulse in the Bio-Z signal were identified using peak detection algorithms. Additionally, a simultaneous measurement was utilized to interpolate the continuous maximum and minimum BP points, with Finapres serving as the reference for the accuracy of the experiments. The estimation of the arterial pulse signal was carried out by a CNN auto-encoder algorithm. Finally, DBP and SBP were estimated using separate regression models based on AdaBoost ensemble learning methods, which predict outcomes by combining multiple weak learners' outputs through a weighted sum of various subsets of the training dataset. Three different methods were employed for training and evaluating the model, differing in data splitting and the number of training samples, achieving significant accuracy that meets the necessary standards for cuffless blood pressure monitors. The Figure 7 shows the proposed model by Ibrahim and Jafari [29]. The SYS (red), DIA (black), and blue point represent the maximum and minimum points indicating systolic, diastolic, and mean pressures, respectively. The array of wristband electrodes and the stages of blood pressure estimation from the obtained signals are displayed.

Griggs et al. [30] designed two models for measuring blood pressure. In the first model, a contact ECG electrode board was used, connected to the bicep muscle, along with a COST PPG sensor attached to the earlobe to record the PPG signal. To pre-amplify the signal, a passive high-pass filter was utilized, and for signal amplification, two low-pass filters OOA333 (TI) were employed. In the second model, a non-contact electrode board (NCE: non contact electrode) was used to record the ECG, which, due to its non-contact nature, is not affected by skin-related factors such as sweat and hair. Additionally, a piezoelectric sensor was used to record pulse pressure, and the INA116 (TI) amplifier was used to amplify these two signals. PPT was used as the first parameter related to blood pressure. Subsequently, to obtain blood pressure, Equations (2)–(4) were created. The variables A and B represent specific constants that affect other biological parameters, such as age, arterial stiffness, and blood density, uniquely for each individual. One of the drawbacks of using PPT is the need for personalization and, in fact, specific calibration for each individual.

$$SBP = \frac{A}{PTT} + B \tag{5}$$

$$SBP = \frac{A}{PTT^2} + B \tag{6}$$

$$SBP = A \times \ln(PTT) + B \tag{7}$$

Considering the long-term use of pressure sensors instead of cuff-based Holters, the design of a cuffless pressure sensor should facilitate easy use in the form of wearable gadgets. Sel et al. [31] utilized a semi-flexible silicone ring to create an appropriate contact surface with the skin, as well as the ease of use in conditions such as sleeping and exercising. They employed a pair of electrodes to inject AC and a Bio-Z sensor to record Bio-Z signals within this ring. Given the limited space for electrode placement compared to the wrist and the impossibility of aligning them in a straight line due to reduced sensitivity, Sel et al. [31] developed a finite element method (FEM) based on the anatomy of the human finger and the tissues of skin, fat, and blood vessels in COMSOL software. From the received Bio-Z signal, features were extracted from each cycle of the Bio-Z waveform, including four categories of characteristics: amplitude values, time intervals, area under the waveform, and gradients calculated from the waveform's derivative, resulting in a total of 15 features for feature extraction. Noise reduction was then performed using a filtering process. The systolic and diastolic blood pressures were estimated using the AdaBoost regression model. The use of these techniques allowed for a measurement range of systolic blood pressure from 89 to 213 mmHg and diastolic pressure from 42 to 122 mmHg. They utilized 5 healthy individuals and 10 potentially healthy individuals during the trial stages, achieving a mean error of 0.11 ± 5.27 for systolic pressure and 0.11 ± 3.87 for diastolic pressure. Figure 8 presents the finite element model and the placement of the electrodes [31]. Part a represents the finite element model of a human finger used in the design of the conductive ring, while part b shows the cross section of four Bio-Z measurement electrodes, with dashed lines indicating the distribution of high-frequency alternating current (AC) in the finger, and the green area representing the sensitive region for

Figure 8
The finite element for the loop

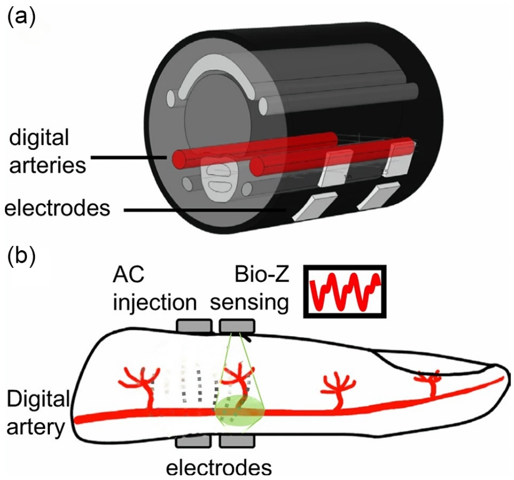

Figure 9
The bioimpedance signal during a cardiac cycle. STT: slope transition time, IBI: inter-beat intervals, A_{dia}: characteristic related to the area between the diastolic point and the slope effect point, A_{slope}: area between the diastolic and systolic points, A_{sys}: systolic point

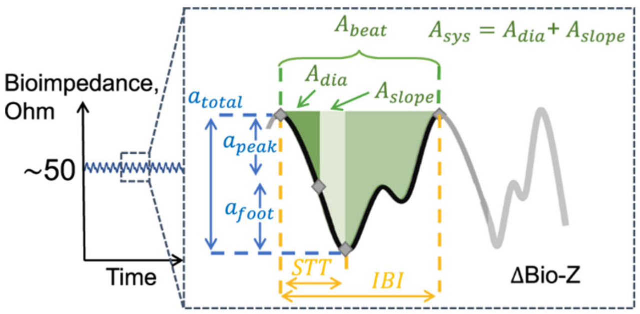

the Bio-Z sensor electrodes. Figure 9 displays a Bio-Z signal over a cardiac cycle [31].

3.2. The estimator of blood pressure

The signals generated by ECG and PPG sensors do not provide direct information about blood pressure; rather, blood pressure must be estimated using signal analysis models based on the characteristics of the relevant signals. One of the primary models used to estimate blood pressure from PPG or ECG signals is the PPT method. The PPT refers to the time it takes for the pressure wave to travel between two points in the artery, where the pressure wave can be observed as a sharp expansion of the artery. Therefore, blood pressure is estimated from the relative timing between the waveforms of the proximal and distal arteries, and PPT has an inverse relationship with blood pressure. This parameter can be obtained by analyzing PPG and ECG signals. One of the most common methods for measuring PPT is to determine the time interval between the R peak of the ECG signal and a specific point in the PPG signal. Furthermore, various relationships for blood pressure, PPT, and other blood-related parameters have been presented, and these relationships are selected based on the available data for each method. It is evident that the more accurate the parameters of these relationships are, the more precise the estimation of blood pressure will be. Griggs et al. [30] used three different relationships to calculate systolic blood pressure in their review of two proposed models, which were mentioned in the previous section. Cattivell and Garudadri [32] provided two relationships (Equations (5) and (6)) for estimating systolic and diastolic blood pressures. In these relationships, HR represents the heart rate, and the coefficients a_1, a_2, b_1, b_2, c_1, and c_2 are obtained through calibration.

$$SBP = a_1 \times PAT + b_1 \times HR + c_1 \tag{8}$$

$$DBP = a_2 \times PAT + b_2 \times HR + c_2 \tag{9}$$

Recently, methods based on ML and DL algorithms for estimating blood pressure from PPG signals have garnered the attention of researchers. Chu et al. [33] utilized a DL model to estimate blood pressure, using data from 1,732 patients obtained from the MIMIC III database. For data preprocessing, flat lines and peaks were selected as outliers and removed using appropriate methods. Additionally, the median was calculated using the Hample filter and replaced the outlier points. The signal was then filtered with a bandpass filter with a frequency range of 0.5 to 8 Hz to help eliminate artifacts and high-frequency noise, and empirical mode decomposition (EMD) was used to remove noise. Finally, the MLM-Transformer model was employed for the final signal processing. The evaluation parameters in this study included the MAE and deviation (MAE±SD) and the squared Pearson correlation coefficient (r^2). The accuracy achieved in this study was compared with the standards of AAMI and the BHS, yielding promising results.

Sammie and Dajani [34] designed a deep neural network for blood pressure estimation based on the morphology of the PPG signal for calibration purposes. They utilized two datasets: the University of Queensland dataset, which included 30 patients, and the University of California, Irvine ML repository, which included 200 patients. In this design, 5 features were used to estimate SBP and 6 features for estimating DBP. Ultimately, they achieved an average error of 0.31. The results from their research indicate that blood pressure estimation based on the morphology of the PPG signal using DL algorithms is a suitable alternative to calibration-dependent methods.

Liu et al. [35] introduced HGCTNet, a hybrid CNN-Transformer model that captures local features (via CNN) and global temporal dependencies (via self-attention). An attention module refines features by removing redundancy, while a fusion module combines them with handcrafted features and demographic data to boost classification performance (Figure 10 [35]).

HGCTNet has been validated on two large datasets, achieving an estimation error of 0.9 ± 6.5 mmHg for diastolic blood pressure and 0.7 ± 8.3 mmHg for systolic blood pressure. These results indicate that the use of DL techniques can significantly enhance the accuracy of blood pressure estimation.

3.3. Results

Overall, the findings obtained from the review of articles are presented in Tables 2 and 3, which focus on the sensor and blood pressure estimation model sections. Additionally, some challenges related to the integration of various types of sensors as the main mechanism for signal acquisition have been gathered.

Figure 10
The HGCTNet hybrid model that includes CNN and Transformer algorithms

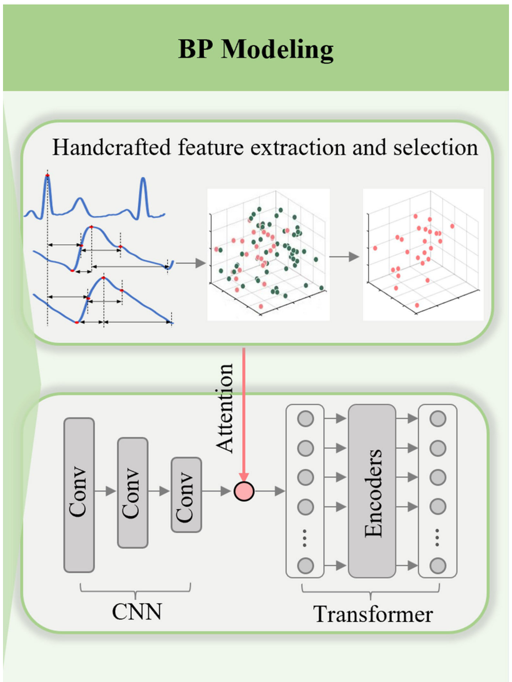

Multimodal sensor fusion has emerged as a promising strategy for cuffless blood pressure monitoring by integrating complementary physiological signals such as PPG, electrocardiogram (ECG), and BioZ. However, the practical realization of this approach faces a range of technical challenges that must be carefully addressed to ensure clinical reliability and usability. A primary challenge lies in the heterogeneous nature of signal acquisition across different sensing modalities. Each modality captures distinct physiological parameters: The PPG reflects peripheral blood volume changes, ECG measures the heart's electrical activity, and BioZ evaluates tissue impedance fluctuations. These signals inherently differ in temporal resolution, sensitivity to artifacts, and noise characteristics. Integrating them into a unified and coherent framework requires advanced synchronization techniques and robust fusion algorithms capable of extracting meaningful features from temporally and functionally dissimilar data sources. Another significant limitation involves motion artifacts and measurement stability, particularly in wearable and ambulatory environments. The PPG signals are highly susceptible to motion-induced distortions and variability due to skin pigmentation. ECG, although less prone to optical interference, depends heavily on consistent skin-electrode contact, which is difficult to maintain over time in wearable designs. Similarly, BioZ measurements are affected by electrode positioning and are prone to baseline drift. These issues collectively reduce the reliability and consistency of blood pressure estimates in real-world settings. Subject-specific variability further complicates the development of generalized models. Anatomical differences between individuals affect signal morphology, and the physiological relationship between derived features—such as PTT—and actual blood pressure is neither stable nor linear across populations. This inter-subject variability is particularly problematic in individuals with cardiovascular abnormalities, often necessitating frequent recalibration to maintain acceptable accuracy. On the hardware side, the integration of multiple sensing components into compact, wearable systems introduces constraints related to size, power consumption, and thermal dissipation. These devices must process high-fidelity signals in real time while preserving battery life, which poses a significant engineering challenge. Furthermore, maintaining signal accuracy and device performance across varying physiological states—such as during exercise, stress, or sleep—adds another layer of complexity. Finally, clinical validation remains a critical barrier. Although multimodal approaches show promise in controlled environments, their reliability under pathological conditions and during acute hemodynamic changes is still uncertain. Short-term variations in cardiovascular parameters introduce additional error sources that are not adequately accounted for in current models. Extensive, diverse clinical trials are required to validate the robustness and safety of these systems before they can be considered for routine medical use. In conclusion, while multimodal sensor fusion represents a compelling avenue for noninvasive and continuous blood pressure monitoring, its clinical translation depends on addressing challenges related to signal heterogeneity, motion robustness, personalization, hardware integration, and rigorous validation. Continued advancements in adaptive signal processing,

Table 2
Summary of the methods reviewed

Author	Materials and Methods Used	Number of Trials	Evaluation Parameters
Ion et al. [22]	Microfluidic with electrolyte liquid	4 electrodes	Sensitivity: 57 ohm/mmHg
Simjanoska et al. [26]	ECG Electrodes	51 cases	Accuracy: 85.71% Error for SBP: 7.86 mmHg Error for DBP: 6 mmHg Correlation coefficient: 0.77
Ibrahim and Jafari [29]	Array of bioimpedance sensors	4 human experiments 12 trials of 90 minutes each (6,000 beats from each person)	Mean error: 0.2
Griggs et al. [30]	ECG + PPG and NCE ECG + Piezoelectric	4 experiments with different scenarios	The relationship between BP inverse PPT or inverse square PPT
Sel et al. [31]	Ring with bioimpedance sensor	5 healthy individuals and 10 possibly healthy individuals	Mean error for SBP: 0.11±5.27 DBP: 0.11±3.87

Table 3
Summary of deep learning approaches for blood pressure estimation

Study	Dataset/Subjects	Methods and Signal Processing	Deep Learning Model	Evaluation Metrics	Results and Accuracy
Chu et al. [33]	MIMIC III/1,732 patients	Outlier removal, Hampel filter, bandpass filtering (0.5–8 Hz), EMD denoising	MLM-Transformer	MAE ± SD, r^2	Complies with AAMI and BHS standards; promising accuracy
Samm and Dajani [34]	University of Queensland (30), UCI ML Repository (200)	PPG morphology-based feature extraction (5 for SBP, 6 for DBP)	Deep neural network (DNN)	Mean error	Avg. error: 0.31; suitable alternative to calibration-based methods
Liu et al. [35]	Two large datasets	CNN for local features, Transformer for temporal context, feature fusion with demographics	HGCTNet (Hybrid CNN-Transformer)	Mean error ± SD	DBP: 0.9 ± 6.5 mmHg, SBP: 0.7 ± 8.3 mmHg; high estimation accuracy

intelligent calibration techniques, and low-power hardware design will be essential to realize the full potential of this technology.

4. Conclusion

Given the importance of blood pressure measurement, researchers in the healthcare field have increased their focus on measuring blood pressure without the use of a cuff. In noninvasive blood pressure measurement without a cuff, two main topics have always been of interest: "the type of sensors used" and "how blood pressure is estimated." When selecting a sensor, considerations should include costs, wearability, and the stability of accuracy and sensitivity of the sensor in various positions. The use of PPG sensors for estimating blood pressure has been of interest in the past; however, due to the lack of robust models, the measurements obtained have not achieved sufficient accuracy. Relying solely on ECG signals is not suitable, as their sensors have limitations, including adequate contact surface. Bio-Z sensors, when designed appropriately and positioned alongside PPG sensors, can be a suitable option for designing a cuffless blood pressure monitor. The use of traditional methods for extracting features from recorded signals, calculating PTT, and estimating blood pressure can be associated with significant errors and, in addition, require calibration and personalization. Nowadays, with the emergence of artificial intelligence and advancements in DL algorithms, the analysis of recorded signals and blood pressure estimation has reached accuracies aligned with existing standards, and the analysis of signals based on their morphology eliminates the need for continuous calibration. Therefore, it is expected that the use of sensors providing information about cardiac activities and the analysis of the resulting signals will become a suitable alternative to cuff-based sphygmomanometers, especially in Holter monitors, and will be utilized in devices such as smartwatches for reporting blood pressure during daily activities.

To advance cuffless blood pressure monitoring, it is recommended to focus on the development of lightweight, low-power, and multimodal sensors that can be easily integrated into wearable devices such as smartwatches. Leveraging DL algorithms to intelligently fuse signals such as PPG, ECG, and BioZ can significantly improve measurement accuracy while reducing the need for frequent calibration. Moreover, large-scale clinical validation across diverse populations with varying physiological conditions is essential to ensure the reliability of these systems in real-world scenarios. Finally, developing signal analysis methods based on morphological features that minimize the dependence on individual calibration could play a key role in enabling the widespread and dependable adoption of this technology in everyday healthcare applications.

Ethical Statement

This study does not contain any studies with human or animal subjects performed by any of the authors.

Conflicts of Interest

The authors declare that they have no conflicts of interest to this work.

Data Availability Statement

Data sharing is not applicable to this article as no new data were created or analyzed in this study.

Author Contribution Statement

Hajar Danesh: Conceptualization and writing – review and editing. **Hamidreza Shirzadfar:** Conceptualization and writing – review and editing. **Mahla Manian:** Investigation and writing – original draft. **Melika Pazhom:** Investigation and writing – original draft.

References

[1] Ventura, H. O., & Lavie, C. J. (2018). Hypertension: Management and measurements. *Current Opinion in Cardiology*, *33*(4), 375–376. https://doi.org/10.1097/HCO.0000000000000534
[2] Dai, D., Ji, Z., & Wang, H. (2024). Non-invasive continuous blood pressure estimation from single-channel PPG based on a temporal convolutional network integrated with an attention mechanism. *Applied Sciences*, *14*(14), 6061. https://doi.org/10.3390/app14146061
[3] Horne, C. E., Stayt, L. C., Schutz, S., Smith, C. M., Haberstroh, A., Bolin, L. P., . . . , & Bibbey, A. (2023). Symptom experiences in hypertension: a mixed methods systematic review. *Journal of Hypertension*, *41*(1), 1–16. https://doi.org/10.1097/hjh.0000000000003306
[4] Wang, A., Tian, X., Zuo, Y., Chen, S., Zhang, Y., Zhang, X., . . . , & Zhou, Y. (2022). Control of blood pressure and risk of

cardiovascular disease and mortality in elderly Chinese: A real-world prospective cohort study. *Hypertension*, *79*(8), 1866–1875. https://doi.org/10.1161/HYPERTENSIONAHA.122.19587

[5] Noh, S. A., Kim, H.-S., Kang, S.-H., Yoon, C.-H., Youn, T.-J., & Chae, I.-H. (2024). History and evolution of blood pressure measurement. *Clinical Hypertension*, *30*(1), 9. https://doi.org/10.1186/s40885-024-00268-7

[6] Al-Qatatsheh, A., Morsi, Y., Zavabeti, A., Zolfagharian, A., Salim, N., Z. Kouzani, A., . . . , & Gharaie, S. (2020). Blood pressure sensors: Materials, fabrication methods, performance evaluations and future perspectives. *Sensors*, *20*(16), 4484. https://doi.org/10.3390/s20164484

[7] Pickering, T. G., Hall, J. E., Appel, L. J., Falkner, B. E., Graves, J., Hill, M. N., . . . , & Roccella, E. J. (2005). Recommendations for blood pressure measurement in humans and experimental animals: Part 1: Blood pressure measurement in humans: A statement for professionals from the subcommittee of professional and public education of the american heart association council on high blood pressure research. *Circulation*, *111*(5), 697–716. https://doi.org/10.1161/01.CIR.0000154900.76284.F6

[8] Shirzadfar, H., Mokhtari, N., & Claudel, J. (2018). Optimize the geometrical parameters of interdigital micro-electrodes used in bioimpedance sensing system. *Journal of Nano- and Electronic Physics*, *10*(5), 05029. https://doi.org/10.21272/jnep.10(5).05029

[9] Nishan, A., Raju, S. T. U., Hossain, M. I., Dipto, S. A., Uddin, S. T., Sijan, A., . . . , & Khan, M. M. H. (2024). A continuous cuffless blood pressure measurement from optimal PPG characteristic features using machine learning algorithms. *Heliyon*, *10*(6), e27779. https://doi.org/10.1016/j.heliyon.2024.e27779

[10] Fortino, G., & Giampa, V. (2010). PPG-based methods for non invasive and continuous blood pressure measurement: An overview and development issues in body sensor networks. In *2010 IEEE International Workshop on Medical Measurements and Applications*, 10–13. https://doi.org/10.1109/MEMEA.2010.5480201

[11] Miao, F., Wen, B., Hu, Z., Fortino, G., Wang, X.-P., Liu, Z.-D., . . . , & Li, Y. (2020). Continuous blood pressure measurement from one-channel electrocardiogram signal using deep-learning techniques. *Artificial Intelligence in Medicine*, *108*, 101919. https://doi.org/10.1016/j.artmed.2020.101919

[12] Bird, K., Chan, G., Lu, H., Greeff, H., Allen, J., Abbott, D., . . . , & Elgendi, M. (2020). Assessment of hypertension using clinical electrocardiogram features: A first-ever review. *Frontiers in Medicine*, *7*, 583331. https://doi.org/10.3389/fmed.2020.583331

[13] Mousavi, S. S., Firouzmand, M., Charmi, M., Hemmati, M., Moghadam, M., & Ghorbani, Y. (2019). Blood pressure estimation from appropriate and inappropriate PPG signals using a whole-based method. *Biomedical Signal Processing and Control*, *47*, 196–206. https://doi.org/10.1016/j.bspc.2018.08.022

[14] Hua, J., Su, M., Wu, J., Zhou, Y., Guo, Y., Shi, Y., & Pan, L. (2024). Wearable cuffless blood pressure monitoring: From flexible electronics to machine learning. *Wearable Electronics*, *1*, 78–90. https://doi.org/10.1016/j.wees.2024.05.004

[15] Fung, P., Dumont, G., Ries, C., Mott, C., & Ansermino, M. (2004). Continuous noninvasive blood pressure measurement by pulse transit time. In *The 26th Annual International Conference of the IEEE Engineering in Medicine and Biology Society*, 738–741. https://doi.org/10.1109/IEMBS.2004.1403264

[16] Yoon, Y., Cho, J. H., & Yoon, G. (2009). Non-constrained blood pressure monitoring using ECG and PPG for personal healthcare. *Journal of Medical Systems*, *33*(4), 261–266. https://doi.org/10.1007/s10916-008-9186-0

[17] Kurylyak, Y., Lamonaca, F., & Grimaldi, D. (2013). A neural network-based method for continuous blood pressure estimation from a PPG signal. In *2022 IEEE International Instrumentation and Measurement Technology Conference*, 280–283. https://doi.org/10.1109/i2mtc.2013.6555424

[18] Sun, S., Bezemer, R., Long, X., Muehlsteff, J., & Aarts, R. M. (2016). Systolic blood pressure estimation using PPG and ECG during physical exercise. *Physiological Measurement*, *37*(12), 2154–2169. https://doi.org/10.1088/0967-3334/37/12/2154

[19] Tanveer, M. S., & Hasan, M. K. (2019). Cuffless blood pressure estimation from electrocardiogram and photoplethysmogram using waveform based ANN-LSTM network. *Biomedical Signal Processing and Control*, *51*, 382–392. https://doi.org/10.1016/j.bspc.2019.02.028

[20] Leitner, J., Chiang, P.-H., & Dey, S. (2022). Personalized blood pressure estimation using photoplethysmography: A transfer learning approach. *IEEE Journal of Biomedical and Health Informatics*, *26*(1), 218–228. https://doi.org/10.1109/JBHI.2021.3085526

[21] Tang, C., Liu, Z., & Li, L. (2022). Mechanical sensors for cardiovascular monitoring: From battery-powered to self-powered. *Biosensors*, *12*(8), 651. https://doi.org/10.3390/bios12080651

[22] Ion, M., Dinulescu, S., Firtat, B., Savin, M., Ionescu, O. N., & Moldovan, C. (2021). Design and fabrication of a new wearable pressure sensor for blood pressure monitoring. *Sensors*, *21*(6), 2075. https://doi.org/10.3390/s21062075

[23] Allen, J. (2007). Photoplethysmography and its application in clinical physiological measurement. *Physiological Measurement*, *28*(3), R1–R39. https://doi.org/10.1088/0967-3334/28/3/R01

[24] Moraes, J. L., Rocha, M. X., Vasconcelos, G. G., Vasconcelos Filho, J. E., de Albuquerque, V. H. C., & Alexandria, A. R. (2018). Advances in photopletysmography signal analysis for biomedical applications. *Sensors*, *18*(6), 1894. https://doi.org/10.3390/s18061894

[25] Kim, K. B., & Baek, H. J. (2023). Photoplethysmography in wearable devices: A comprehensive review of technological advances, current challenges, and future directions. *Electronics*, *12*(13), 2923. https://doi.org/10.3390/electronics12132923

[26] Simjanoska, M., Gjoreski, M., Gams, M., & Madevska Bogdanova, A. (2018). Non-invasive blood pressure estimation from ECG using machine learning techniques. *Sensors*, *18*(4), 1160. https://doi.org/10.3390/s18041160

[27] Craig Herndon, R. (2021). Determining signal entropy in uncertainty space. *Measurement*, *178*, 109336. https://doi.org/10.1016/j.measurement.2021.109336

[28] Motamedi-Fakhr, S., Moshrefi-Torbati, M., Hill, M., Hill, C. M., & White, P. R. (2014). Signal processing techniques applied to human sleep EEG signals—A review. *Biomedical Signal Processing and Control*, *10*, 21–33. https://doi.org/10.1016/j.bspc.2013.12.003

[29] Ibrahim, B., & Jafari, R. (2022). Cuffless blood pressure monitoring from a wristband with calibration-free algorithms for sensing location based on bio-impedance sensor array

and autoencoder. *Scientific Reports*, *12*(1), 319. https://doi.org/10.1038/s41598-021-03612-1

[30] Griggs, D., Sharma, M., Naghibi, A., Wallin, C., Ho, V., Barbosa, K., . . . , & Krishnan, S. K. (2016). Design and development of continuous cuff-less blood pressure monitoring devices. In *2016 IEEE Sensors*, 1–3. https://doi.org/10.1109/ICSENS.2016.7808908

[31] Sel, K., Osman, D., Huerta, N., Edgar, A., Pettigrew, R. I., & Jafari, R. (2023). Continuous cuffless blood pressure monitoring with a wearable ring bioimpedance device. *Npj Digital Medicine*, *6*(1), 59. https://doi.org/10.1038/s41746-023-00796-w

[32] Cattivelli, F. S., & Garudadri, H. (2009). Noninvasive cuffless estimation of blood pressure from pulse arrival time and heart rate with adaptive calibration. In *2009 Sixth International Workshop on Wearable and Implantable Body Sensor Networks*, 114–119. https://doi.org/10.1109/BSN.2009.35

[33] Chu, Y., Tang, K., Hsu, Y.-C., Huang, T., Wang, D., Li, W., . . . , & Shams, S. (2023). Non-invasive arterial blood pressure measurement and SpO_2 estimation using PPG signal: A deep learning framework. *BMC Medical Informatics and Decision Making*, *23*(1), 131. https://doi.org/10.1186/s12911-023-02215-2

[34] Samimi, H., & Dajani, H. R. (2023). A PPG-based calibration-free cuffless blood pressure estimation method using cardiovascular dynamics. *Sensors*, *23*(8), 4145. https://doi.org/10.3390/s23084145

[35] Liu, Z.-D., Li, Y., Zhang, Y.-T., Zeng, J., Chen, Z.-X., Liu, J.-K., & Miao, F. (2024). HGCTNet: Handcrafted feature-guided CNN and transformer network for wearable cuffless blood pressure measurement. *IEEE Journal of Biomedical and Health Informatics*, *28*(7), 3882–3894. https://doi.org/10.1109/JBHI.2024.3395445

How to Cite: Danesh, H., Shirzadfar, H., Manian, M., & Pazhom, M. (2025). The Recent Advancements to Measure the Blood Pressure Using Photoplethysmography, Electrocardiogram, and Microchannel. *Smart Wearable Technology*. https://doi.org/10.47852/bonviewSWT52026420